

Neural Network Based in Silico Simulation of Combustion Reactions

Jinze Zeng¹, Liqun Cao¹, Mingyuan Xu¹, Tong Zhu^{1,2,*} and John ZH Zhang^{1,2,3*}

¹ Shanghai Engineering Research Center of Molecular Therapeutics & New Drug Development, School of Chemistry and Molecular Engineering, East China Normal University, Shanghai, 200062, China

²NYU-ECNU Center for Computational Chemistry at NYU Shanghai, Shanghai, 200062, China

³Department of Chemistry, New York University, New York 10003, United States

Email: tzhu@lps.ecnu.edu.cn, john.zhang@nyu.edu

Abstract: Understanding and prediction of the chemical reactions are fundamental demanding in the study of many complex chemical systems. Reactive molecular dynamics (MD) simulation has been widely used for this purpose as it can offer atomic details and can help us better interpret chemical reaction mechanisms. In this study, two reference datasets were constructed and corresponding neural network (NN) potentials were trained based on them. For given large-scale reaction systems, the NN potentials can predict the potential energy and atomic forces of DFT precision, while it is orders of magnitude faster than the conventional DFT calculation. With these two models, reactive MD simulations were performed to explore the combustion mechanisms of hydrogen and methane. Benefit from the high efficiency of the NN model, nanosecond MD trajectories for large-scale systems containing hundreds of atoms were produced and detailed combustion mechanism was obtained. Through further development, the algorithms in this study can be used to explore and discovery reaction mechanisms of many complex reaction systems, such as combustion, synthesis, and heterogeneous catalysis without any predefined reaction coordinates and elementary reaction steps.

Understanding and prediction of chemical reactions are the fundamental demanding in the study of many complex chemical systems such as combustion, catalysis, and synthesis. Limited by the resolution of experimental detection methods, direct experimental characterization of a chemical reaction is extremely challenging. In the past decades, reactive molecular dynamics (MD) simulations have shown their value in providing molecular-level insights into the mechanism of chemical reactions for a series of systems. Compared to experiments, MD simulations can observe all the details of the reaction from different perspectives. In addition, the reaction conditions can be easily controlled in the simulation, some supercritical conditions which are difficult to achieve in the experiment can also be handled.

The heart of the reactive MD simulation is the potential energy surface (PES) which describes the inter- and intramolecular interactions in the system. Currently, there are mainly two classes of methods that can be used to construct the PES of a given molecular system: the quantum mechanics (QM)-based methods and the empirical force fields. Quantum mechanics is undoubtedly more rigorous and accurate, and MD simulations based on it are also known as *ab initio* MD simulation (AIMD)¹. Unfortunately, the computational cost inherent in the QM calculation severely limits the simulation scale of the AIMD method. Usually, it can only handle simulations of systems containing no more than atoms in a picosecond time scale. With the rapid development of computer hardware and algorithms, especially the employment of graphic processing units (GPUs), some AIMD methods have recently begun to handle larger chemical systems². But so far, it is still unrealistic to use AIMD to simulate large-scale reaction molecular systems.

Compared with QM calculation, the efficiency of empirical reactive force fields such as ReaxFF^{3, 4, 5, 6, 7}, REBO⁸, and MEAM⁹ are much higher, making it possible to reach simulation scales that are orders of magnitude beyond what is tractable for conventional AIMD methods^{10, 11}. However, efficiency is not a free lunch. Many previous studies have questioned the accuracy of empirical reactive force fields^{12, 13, 14}. The most difficult part of developing a reaction force field is the choice of function form, which should accurately describe the various important interactions in the chemical system, especially the breaking and formation of chemical bonds. In addition, the complicated parameterization process also hinders the development of reactive force fields.

Recently, more and more researchers are switching to seek the help of machine learning (ML) methods. ML methods, especially artificial neural networks (NN), provided the possibility to construct PESs with the accuracy of the QM method while its efficiency is as high as to force fields. Neural networks constitute a very

flexible and unbiased class of mathematical functions, which in principle is able to approximate any real-valued function to arbitrary accuracy. Since Behler and Parrinello proposed the high-dimensional neural network (HDNN) approach^{15, 16, 17, 18, 19, 20}, many different NN PESs have been proposed for water, small organic molecules and metal materials. For example, the sGDML and DTNN of Müller et al.^{21, 22, 23}, the kCON model of Hammer et al.²⁴, and the DeepMD method of Wang and co-workers^{25, 26}. NN potentials have also been employed to study the reaction mechanisms of chemical systems. By combining high-precision NN PESs and quantum dynamics method, Zhang and Jiang's group have studied a series of elementary reactions in the gas phase and on the surface^{27, 28, 29, 30}. Liu and co-workers developed the LASP program to study the heterogeneous catalysis with NN PESs³¹. Meuwly et. al also studied the nucleophilic substitution reaction $[\text{Cl}-\text{CH}_3-\text{Br}]^-$ in water with NN potential³².

To date, NN PESs have only been used to study the reaction mechanisms of small or medium-sized molecular systems, while its performance in large complex reaction systems is not known. In this work, a workflow of preparing reference datasets with a machine learning approach was proposed. Then two NN PESs were trained and used to simulate the oxidization of hydrogen and methane. The potential energy and atomic forces can be accurately predicted by the NN PESs, and benefit from their high efficiency, sub-nanosecond MD trajectories for systems containing hundreds to thousands of atoms were produced. Based on the simulation, detailed combustion mechanisms were obtained and are highly consistent with the experiments.

Results

Accuracy of NN PESs. The performance of the NN potential highly depends on the quality of the reference datasets. Although there are several databases, such as QM7³³, QM9³⁴, ANI-1³⁵, and ANI-1x³⁶, are accessible, they mainly include organic molecules and are therefore not suitable for this work. Combustion will produce a lot of molecular fragments and most of them are free radicals³⁷. Therefore, we proposed a workflow (details are listed in the Methodology section) to construct the reference datasets for the combustion. Then the DeepPot-SE model³⁸ was used to train two NN PESs based on the reference datasets for the hydrogen- and methane-combustion system (For the sake of convenience, we call them H₂-system and the CH₄-system, respectively). The mean absolute errors (MAEs) and root mean squared errors (RMSEs) of total energies are shown in Table 1. It is clear that DFT energies are accurately reproduced. For the H₂-system, the MAE and RMSE are only 0.058eV/atom and 0.099eV/atom in the test set. While for the CH₄-system, the errors of energy

are slightly larger (the RMSE are 0.14eV/atom and 0.24eV/atom in the training set and test set, respectively.) than that of H₂-system, but still very small.

Table 1. Energy prediction errors for the hydrogen and methane dataset. The mean absolute errors (MAEs) and root mean squared errors (RMSEs) are in eV/atom.

System	Training Set / Test Set		
	Structure Number	MAE	RMSE
Hydrogen	136,910/4,471	0.016/0.058	0.027/0.099
Methane	578,731/13,315	0.041/0.140	0.073/0.240

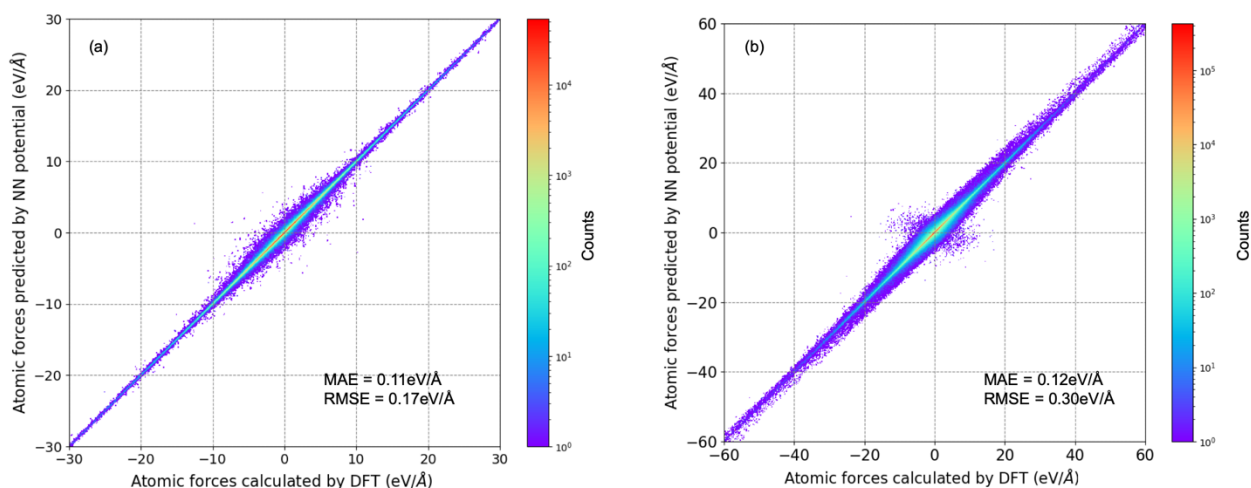


Figure 1. The correlation of atomic forces between NN predictions and DFT calculations. (a), results of the H₂-system; (b), results of the CH₄-system.

As for the atomic forces, the predicted values of the NN models are also highly consistent with the calculated results of the DFT (Fig. 1). The correlation coefficients are 0.999 and 0.999, respectively. And the RMSEs of both systems are within 10 kcal/(mol·Å). Considering that there are a large number of atomic collisions during the combustion, and some atomic forces can be as high as hundreds of eV/Å, the accuracy of these two models is encouraging.

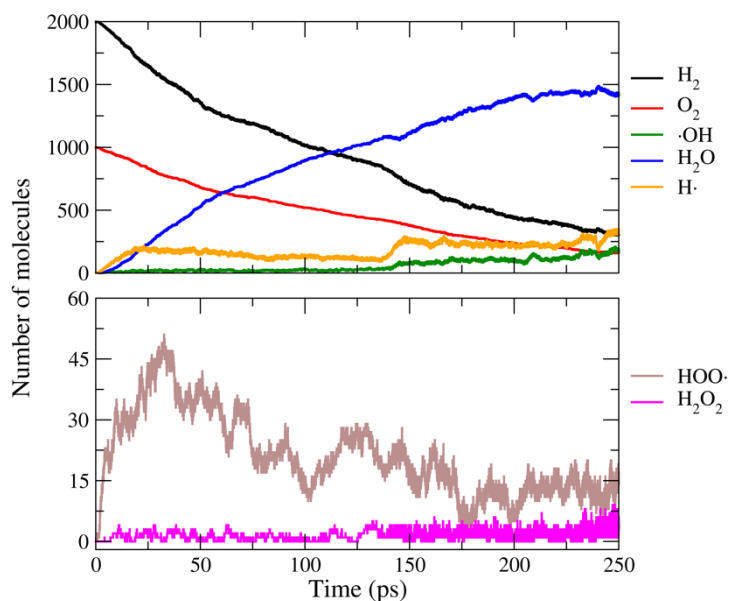


Figure 2. Major species generated during the simulation of H₂-system.

The combustion of hydrogen gas. A 250ps reactive MD simulation was performed for hydrogen combustion with the NN PES by LAMMPS package³⁹. The system is a period box contains 2000 H₂ molecules and 1000 O₂ molecules, whose density is 0.25 g/cm³. NVT MD simulations were performed with a time step of 0.1fs, the temperature was kept at 3000K by using the Berendsen thermostat. Fig. 2 shows the major species generated during the simulation, which include the reactants, two products (H₂O and HOOH), and three active species ·HO₂, HO·, and H·. As can be seen, the product is rapidly produced while the reactants are being consumed. After 250ps, most of H₂ and O₂ are consumed and 1418 water molecules are generated.

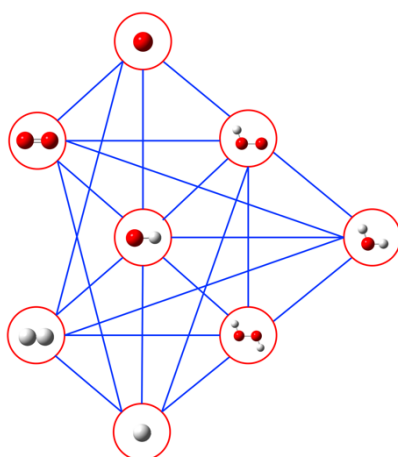


Figure 3. Reaction network for hydrogen combustion.

The most important reason for reactive MD simulations of chemical reaction systems is to determine the reaction mechanism. To this end, we analyzed the trajectory with the help of ReacNetGenerator⁴⁰. Fig. 3 shows

a reaction network diagram detected from the trajectory. The species types and the relationship between them are basically in line with the experiments^{41, 42, 43, 44} and previous theoretical studies⁴⁵. The further careful analysis found that the collision of H₂ and O₂ can generate H·, O·, HO·, and ·HO₂:



Then the HO· and ·HO₂ can participate in free radical reactions:



And water molecules are mainly produced by the following reactions:



These reactions can all be found in the previous theory study⁴⁴ and experimental measurements^{41, 42, 43, 44}, which indicates the success of the NN PESs for the H₂-system.

The combustion of methane. A 500ps reactive MD simulation was performed for methane combustion with the NN PES. The system contains 100 CH₄ molecules and 200 O₂ molecules (a total of 900 atoms). The density is also 0.25 g/cm³. Other simulation conditions are the same as that of H₂.

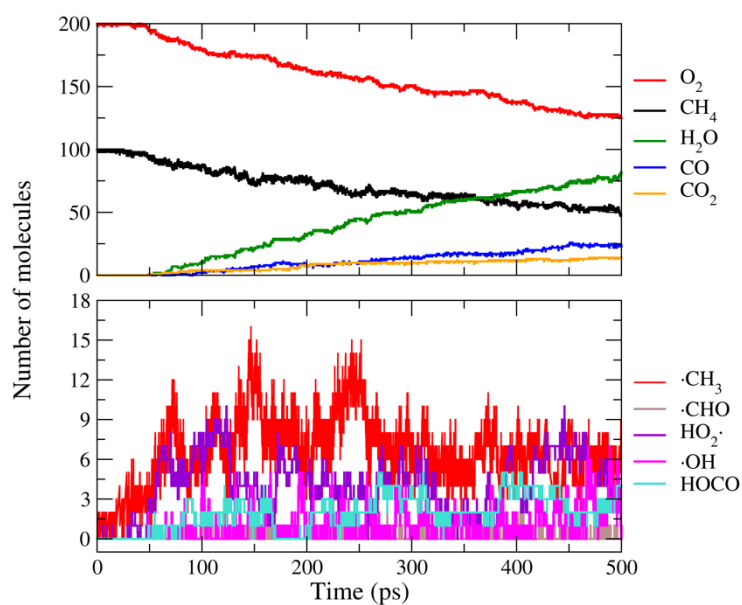


Figure 4. Major species generated during the simulation of CH₄-system.

Fig. 4 show the changes of the main species during the MD simulation. Similarly, as the H₂-system, some expecting (which are important) molecules and free radicals appear in the trajectory. After 500ps simulation, about 50 CH₄ and 100 O₂ are consumed. More than 140 species and 400 reactions are observed and about 80 H₂O, 25 CO, and 15 CO₂ are produced. The main reaction routes are shown in Fig. 5. The combustion of methane starts with the abstraction of the H atom from the CH₄ by O₂, and two free radicals, ·CH₃ and ·HO₂, will be produced. During the simulation, other radicals such as ·H, ·OH, and ·HO₂ can also abstract H atom from CH₄ and form ·CH₃. The atomization of methane into ·H and ·CH₃ was also observed.

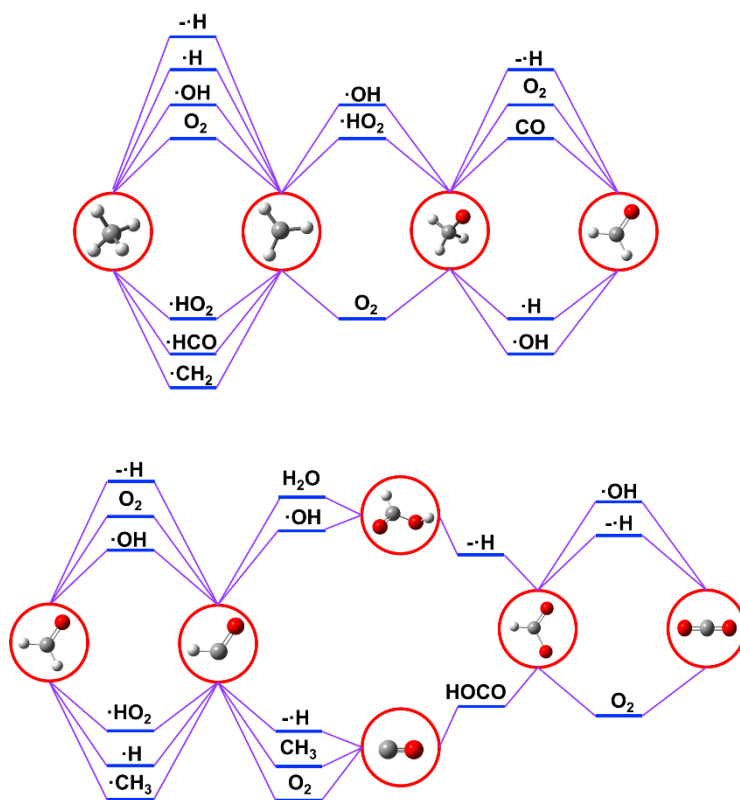


Figure 5. Main reaction routes in the simulation methane oxidation with NN PES.

Then the $\cdot\text{CH}_3$ radicals interacted with $\cdot\text{HO}_2$, $\cdot\text{OH}$ and O_2 to form the $\text{CH}_3\text{O}\cdot$ radicals. Then the $\text{CH}_3\text{O}\cdot$ radicals were abstracted hydrogen atoms by $\cdot\text{H}$, $\cdot\text{OH}$, O_2 , and CO to form formaldehyde molecules. The $\text{CH}_3\text{O}\cdot$ radicals can also be transformed into $\cdot\text{CH}_2\text{OH}$, and then produce formaldehyde by losing a hydrogen atom.

The formaldehydes were further converted into the formyl ($\text{HCO}\cdot$) radicals. The main reaction paths are hydrogen abstraction by $\cdot\text{H}$, $\cdot\text{OH}$, O_2 , $\cdot\text{HO}_2$, and $\cdot\text{CH}_3$. The formyl radical can subsequently lose a hydrogen atom via reactions, thereby forming the carbon monoxide (CO). It can also interact with $\cdot\text{OH}$ and H_2O to form the HCOOH molecule and further convert into the $\cdot\text{CO}_2\text{H}$ radicals, which can be further converted to carbon dioxide. These reactions are consistent with the previous study³⁷ and experiments⁴⁶.

Discussion

In this work, two neural networks PESs are trained to describe the complex interactions in the combustion of hydrogen and methane, including the forming and breaking of chemical bonds. These NN models can predict the potential energy and atomic forces of DFT precision, while it is orders of magnitude faster than the

conventional DFT calculation. With these two models, reactive MD simulations were performed to explore the combustion mechanisms of hydrogen and methane. Benefit from their high efficiency, nanosecond-scale MD simulations for chemical systems that contain nearly one thousand atoms can be achieved in a week or so. Detailed reaction mechanisms were extracted from the trajectory, which showed excellent agreement with the experiments. Compared to classical force fields, these neural network potentials are not limited by the form of potential function and the complicated parameterization process.

One might concern that a cutoff was used in the training of NN PESs, which means that the interaction between two atoms will be ignored if their distance is larger than the cutoff. This may be a critical issue in condensed matter systems, but gas-phase reactions like combustion are dominated by collisions between molecules, the contribution of long-range interactions to reactions in such a system should be negligibly small (Figure S1.) Another issue to be pointed out is that, although some algorithms were used in this study to minimize the size of the reference dataset, there are still 578,731 structures in the training set of CH₄-system, which will consume a lot of computational resources for QM calculation. In order to further minimize the size of the reference set while ensuring its completeness, new algorithms still need to be developed. Many pioneers have come up with some solutions, such as active learning and more complex clustering algorithms, and we are also working on this problem.

However, these issues cannot conceal the bright future of the application of NN-based reactive MD simulation in studying the reaction mechanism of large-scale chemical systems. Through further development, the algorithms in this study can be used to explore and discovery reaction mechanisms of many complex reaction systems, such as combustion, synthesis, and heterogeneous catalysis without any predefined reaction coordinates and elementary reaction steps.

Methodology

Reference dataset. In this study, a workflow was proposed for making reference datasets:

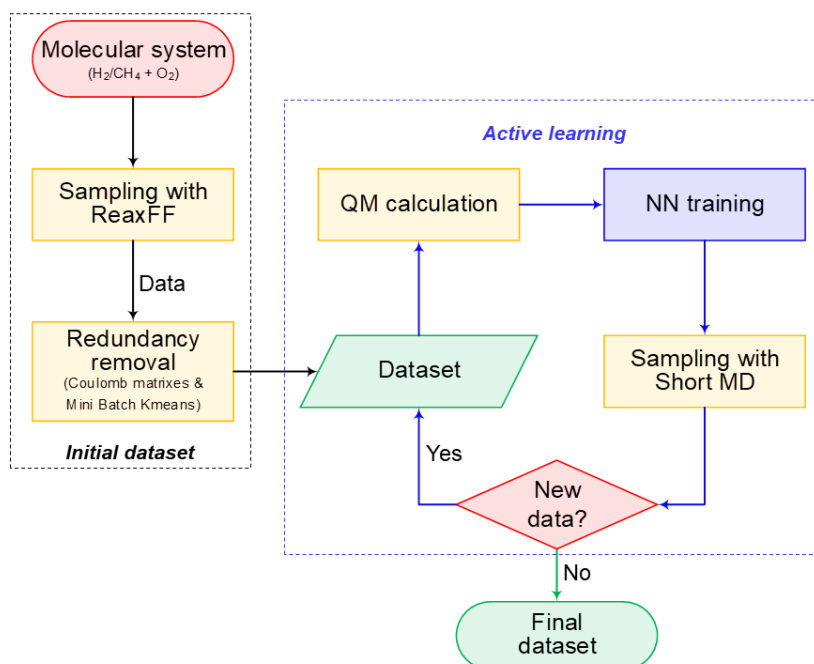


Figure 6. The workflow of reference dataset construction.

The details of each module in the workflow are given below.

Reactive MD simulation with ReaxFF. Reactive MD simulation with ReaxFF was used to sample the initial dataset. Two molecular systems for the oxidation of hydrogen and methane were built by using the Amorphous Cell module in Material Studio⁴⁷. The hydrogen oxidation system contains 500 hydrogen molecules and 250 oxygen molecules while the methane oxidation system contains 500 methane molecules and 1000 oxygen molecules. The densities of these two systems were set to 0.25g/cm³. The Forcite module in Materials Studio was used to equilibrate these two systems at 298K for 250ps. Then the LAMMPS⁴⁸ program was used to perform the MD simulation for 250ps (H₂-system) and 2500ps (CH₄-system). The NVT ensemble was used and the temperature was set to 3000K with the Berendsen thermostat. The ReaxFF parameter of Chenoweth et al. (CHO-2008 parameter set)⁴⁹ was employed. The time step of the simulation was 0.1fs and the atomic coordination was recorded every 10fs.

The initial dataset. For the H₂- and CH₄-system, we got 0.25ns and 2.5ns trajectories, respectively. The Open Babel software⁵⁰ and the Depth-First Search algorithm⁵¹ were used to detect species in every snapshot of the trajectory. Then, for each atom in each snapshot, we build a molecular cluster that contains this atom and

species that within a specified cutoff centered on it. In this work, the cutoff was set to 5Å. The initial dataset for H₂-system contains about 15 million structures, while there are about 22.5 million structures in the CH₄-system.

Redundancy removal. The initial training sets are too large to perform QM calculations for every molecular cluster it contains. Therefore, it is necessary to resample it to remove redundant structures while ensuring its completeness. To this end, we first classified the initial training sets into sub-datasets based on the chemical bond information of the central atom. For example, the central H atom can be classified into 2 different types: a single H atom (H0) and an H atom formed a single chemical bond with another atom (H1).

Further treatment still needed for large sub-datasets. For a given large sub-dataset, we first expressed each molecular cluster it contains as a Coulomb matrix⁵²:

$$\mathbf{C}_{ij} = \begin{cases} \frac{1}{2}Z_i^{2.4}, & i = j \\ \frac{Z_i Z_j}{|R_i - R_j|}, & i \neq j \end{cases} \quad (1).$$

Where Z_i and Z_j are nuclear charges of atom i and j , \mathbf{R}_i and \mathbf{R}_j are their Cartesian coordinates. The minimum image convention⁵³ was used to consider the periodic boundary condition. “Invisible atoms” were introduced to fix the dimension of the Coulomb matrix. These invisible atoms do not influence the physics of the molecule of interest and make the total number of atoms in the molecule sum to a constant. To lower the dimension of the dataset and keep as much structural information as possible, the Coulomb matrix was further represented by the eigen-spectrum, which is obtained by solving the eigenvalue problem $\mathbf{C}\mathbf{v} = \lambda\mathbf{v}$ under the constraint $\lambda_i \geq \lambda_{i+1}$.

Then the clustering algorithm Mini Batch KMeans⁵⁴, was used to cluster the given sub-datasets into smaller clusters according to the eigen-spectrum. Then we randomly selected 10000 structures from each cluster (If the cluster contains no more than 10000 structures, then all of them were selected).

After the redundancy removal process, the dataset of the H₂-system contains 136,910 structures while there are 578,031 structures in the dataset of CH₄-system.

Active learning. Large amplitude collisions and reactions in the combustion can produce a lot of unpredictable species and intermediates. To ensure the completeness of the reference dataset, an active learning approach⁵⁵ was used. Four different NN PES models were trained based on the dataset from the last step. Then several short MD simulations were performed. During the simulation, the atomic forces are evaluated by these

four NN PES models simultaneously. For a specific atom, if the predicted forces by these four models are consistent with each other, then the molecular cluster which centered on this atom can be found in the dataset. On the contrary, if the results of these four models are inconsistent with each other and the error between them is in a specific range ($0.5\text{eV}/\text{\AA} < \text{error} < 1.0\text{eV}/\text{\AA}$ in this work), the corresponding molecular cluster will be added into the dataset. This process will be continued until the predictions of the four models are always consistent.

QM calculation. The potential energy and atomic forces for every structure in the final dataset were calculated by Gaussian 16⁵⁶ software at the MN15/6-31g** level. The MN15 functional was employed because of its good performance on multiconfigurational systems⁵⁷. To consider the spin polarization effect, the initial wave function of a given structure is obtained by the combination of the wave functions of species that make up it. While the wave functions of the species are obtained based on their charge and spin.

Training of the NN PES. The DeepPot-SE (Deep Potential - Smooth Edition) model³⁸ was used to train the NN potential by DeePMD-kit program⁵⁸. Details of this method can be found in Ref. (57). For both systems, the model includes two networks: the embedding network and the fitting network. Both networks use ResNet architecture⁵⁹. The embedding network was set to (25, 50, 100) and the size of the embedding matrix was set to 12. The size of the fitting network is set to 240, 240, 240 and a timestep is used in the ResNet. The cutoff radius was set to 6.0\AA and the descriptors decay smoothly from 1.0\AA to 6.0\AA . The initial learning rate was set to 0.0005 and it will decay every 20000 steps. The loss is defined by

$$\mathcal{L} = p_e \mathcal{L}_e + p_f \mathcal{L}_f \quad (2)$$

where the prefactor of the energy error \mathcal{L}_e is set to 0.2 eV^{-1} and the prefactor of force error \mathcal{L}_f decays from $1000\text{\AA}\cdot\text{eV}^{-1}$ to $1\text{\AA}\cdot\text{eV}^{-1}$.

Conflicts of interest

There are no conflicts to declare.

Corresponding Author

*E-mail: tzhu@lps.ecnu.edu.cn

*E-mail: jz2@nyu.edu

Acknowledgments

The author thanks Mr. Linfeng Zhang and Dr. Han Wang for their discussion and help in using DeepPot-SE, DeePMD-kit. T. Zhu would also like to thank Prof. Donghui Zhang for his valuable suggestions in this project.

This work was supported by the National Natural Science Foundation of China (Grants No. 91641116). J. Zeng was partially supported by the National Innovation and Entrepreneurship Training Program for Undergraduate (201910269080). We also thank the ECNU Multifunctional Platform for Innovation (No. 001) for providing supercomputer time.

References

1. Tuckerman ME. Ab initio molecular dynamics: basic concepts, current trends and novel applications. *J Phys: Condens Matter* **14**, R1297-R1355 (2002).
2. Wang L-P, Titov A, McGibbon R, Liu F, Pande VS, Martínez TJ. Discovering chemistry with an ab initio nanoreactor. *Nature Chem* **6**, 1044 (2014).
3. Van Duin AC, Dasgupta S, Lorant F, Goddard WA. ReaxFF: a reactive force field for hydrocarbons. *J Phys Chem A* **105**, 9396-9409 (2001).
4. van Duin AC, Zeiri Y, Dubnikova F, Kosloff R, Goddard WA. Atomistic-scale simulations of the initial chemical events in the thermal initiation of triacetone triperoxide. *J Am Chem Soc* **127**, 11053-11062 (2005).
5. Strachan A, Kober E, Adri CT van Duin, J. Oxgaard, and WA Goddard III. *J Chem Phys* **122**, 054502 (2005).
6. Strachan A, van Duin AC, Chakraborty D, Dasgupta S, Goddard III WA. Shock waves in high-energy materials: The initial chemical events in nitramine RDX. *Phys Rev Lett* **91**, 098301 (2003).
7. Chenoweth K, Cheung S, Van Duin AC, Goddard WA, Kober EM. Simulations on the thermal decomposition of a poly (dimethylsiloxane) polymer using the ReaxFF reactive force field. *J Am Chem Soc* **127**, 7192-7202 (2005).
8. Brenner DW, Shenderova OA, Harrison JA, Stuart SJ, Ni B, Sinnott SB. A second-generation reactive empirical bond order (REBO) potential energy expression for hydrocarbons. *J Phys: Condens Matter* **14**, 783 (2002).
9. Nouranian S, Tschopp MA, Gwaltney SR, Baskes MI, Horstemeyer MF. An interatomic potential for saturated hydrocarbons based on the modified embedded-atom method. *Phys Chem Chem Phys* **16**, 6233-6249 (2014).
10. Zheng M, *et al.* Pyrolysis of Liulin Coal Simulated by GPU-Based ReaxFF MD with Cheminformatics Analysis. *Energy Fuels* **28**, 522-534 (2014).
11. Han S, Li X, Nie F, Zheng M, Liu X, Guo L. Revealing the Initial Chemistry of Soot Nanoparticle Formation by ReaxFF Molecular Dynamics Simulations. *Energy Fuels* **31**, 8434-8444 (2017).
12. Wang E, Ding J, Qu Z, Han K. Development of a Reactive Force Field for Hydrocarbons and Application to Iso-octane Thermal Decomposition. *Energy Fuels* **32**, 901-907 (2017).
13. Koziol L, Fried LE, Goldman N. Using Force Matching To Determine Reactive Force Fields for Water under Extreme Thermodynamic Conditions. *J Chem Theory Comput* **13**, 135-146 (2017).
14. Cheng T, Jaramillo-Botero A, Goddard WA, Sun H. Adaptive Accelerated ReaxFF Reactive Dynamics with Validation from Simulating Hydrogen Combustion. *J Am Chem Soc* **136**, 9434-9442 (2014).
15. Behler J, Parrinello M. Generalized neural-network representation of high-dimensional potential-energy surfaces. *Phys Rev Lett* **98**, 146401 (2007).

16. Behler J. Neural network potential-energy surfaces in chemistry: a tool for large-scale simulations. *Phys Chem Chem Phys* **13**, 17930-17955 (2011).
17. Behler J. Atom-centered symmetry functions for constructing high-dimensional neural network potentials. *J Chem Phys* **134**, 074106 (2011).
18. Morawietz T, Sharma V, Behler J. A neural network potential-energy surface for the water dimer based on environment-dependent atomic energies and charges. *J Chem Phys* **136**, 064103 (2012).
19. Behler J. First Principles Neural Network Potentials for Reactive Simulations of Large Molecular and Condensed Systems. *Angew Chem Int Ed Engl* **56**, 12828-12840 (2017).
20. Nguyen TT, *et al.* Comparison of permutationally invariant polynomials, neural networks, and Gaussian approximation potentials in representing water interactions through many-body expansions. *J Chem Phys* **148**, (2018).
21. Chmiela S, Tkatchenko A, Sauceda HE, Poltavsky I, Schutt KT, Muller KR. Machine learning of accurate energy-conserving molecular force fields. *Science Advances* **3**, e1603015 (2017).
22. Schutt KT, Arbabzadah F, Chmiela S, Muller KR, Tkatchenko A. Quantum-chemical insights from deep tensor neural networks. *Nature Communications* **8**, 13890 (2017).
23. Sauceda HE, Chmiela S, Poltavsky I, Muller KR, Tkatchenko A. Molecular force fields with gradient-domain machine learning: Construction and application to dynamics of small molecules with coupled cluster forces. *J Chem Phys* **150**, 114102 (2019).
24. Chen X, Jørgensen MS, Li J, Hammer B. Atomic energies from a convolutional neural network. *J Chem Theory Comput* **14**, 3933-3942 (2018).
25. Zhang L, Han J, Wang H, Car R, Weinan E. Deep potential molecular dynamics: a scalable model with the accuracy of quantum mechanics. *Phys Rev Lett* **120**, 143001 (2018).
26. Han JQ, Zhang LF, Car R, Weinan E. Deep Potential: A General Representation of a Many-Body Potential Energy Surface. *Communications in Computational Physics* **23**, 629-639 (2018).
27. Lu X, Meng Q, Wang X, Fu B, Zhang DH. Rate coefficients of the $H+H_2O_2 \rightarrow H_2+HO_2$ reaction on an accurate fundamental invariant-neural network potential energy surface. *J Chem Phys* **149**, 174303 (2018).
28. Yin Z, Guan Y, Fu B, Zhang DH. Two-state diabatic potential energy surfaces of CIH 2 based on nonadiabatic couplings with neural networks. *Phys Chem Chem Phys* **21**, 20372-20383 (2019).
29. Zhang Y, Hu C, Jiang B. Embedded Atom Neural Network Potentials: Efficient and Accurate Machine Learning with a Physically Inspired Representation. *J Phys Chem Lett* **10**, 4962-4967 (2019).
30. Zhang Y, Zhou X, Jiang B. Bridging the gap between direct dynamics and globally accurate reactive potential

- energy surfaces using neural networks. *J Phys Chem Lett* **10**, 1185-1191 (2019).
31. Huang SD, Shang C, Kang PL, Zhang XJ, Liu ZP. LASP: Fast global potential energy surface exploration. *Wiley Interdisciplinary Reviews: Computational Molecular Science*, e1415 (2019).
 32. Brickel S, Das AK, Unke OT, Turan HT, Meuwly M. Reactive molecular dynamics for the [Cl-CH₃-Br]-reaction in the gas phase and in solution: a comparative study using empirical and neural network force fields. *Electronic Structure* **1**, 024002 (2019).
 33. Blum LC, Raymond J-L. 970 million druglike small molecules for virtual screening in the chemical universe database GDB-13. *J Am Chem Soc* **131**, 8732-8733 (2009).
 34. Ruddigkeit L, Van Deursen R, Blum LC, Raymond J-L. Enumeration of 166 billion organic small molecules in the chemical universe database GDB-17. *J Chem Inf Model* **52**, 2864-2875 (2012).
 35. Smith JS, Isayev O, Roitberg AE. ANI-1, A data set of 20 million calculated off-equilibrium conformations for organic molecules. *Scientific data* **4**, 170193 (2017).
 36. Smith JS, *et al.* The ANI-1ccx and ANI-1x data sets, coupled-cluster and density functional theory properties for molecules. 10.26434/chemrxiv.10050737.v1 (2019).
 37. He Z, Li X-B, Liu L-M, Zhu W. The intrinsic mechanism of methane oxidation under explosion condition: A combined ReaxFF and DFT study. *Fuel* **124**, 85-90 (2014).
 38. Zhang L, Han J, Wang H, Saidi WA, Car R. End-to-end Symmetry Preserving Inter-atomic Potential Energy Model for Finite and Extended Systems. *arXiv preprint arXiv:180509003*, (2018).
 39. Plimpton S. Fast parallel algorithms for short-range molecular dynamics. *J Comput Phys* **117**, 1-19 (1995).
 40. Zeng J, Cao L, Chin C-H, Ren H, Zhang JZ, Zhu T. ReacNetGenerator: an Automatic Reaction Network Generator for Reactive Molecular Dynamic Simulations. *Phys Chem Chem Phys*, (2019).
 41. Olm C, *et al.* Comparison of the performance of several recent hydrogen combustion mechanisms. *Combust Flame* **161**, 2219-2234 (2014).
 42. Das L. On-board hydrogen storage systems for automotive application. *Int J Hydrogen Energy* **21**, 789-800 (1996).
 43. Brabbs TA, Lezberg EA, Bittker DA, Robertson TF. Hydrogen oxidation mechanism with applications to (1) the Chaperon efficiency of carbon dioxide and (2) vitiated air testing. (1987).
 44. Varga T, *et al.* Optimization of a hydrogen combustion mechanism using both direct and indirect measurements. In: *Proceedings of the Combustion Institute* **33**, 589-596 (2015).
 45. Cheng T, Jaramillo-Botero As, Goddard III WA, Sun H. Adaptive accelerated ReaxFF reactive dynamics with

- validation from simulating hydrogen combustion. *J Am Chem Soc* **136**, 9434-9442 (2014).
46. Gregory P. Smith DMG, Michael Frenklach, Nigel W. Moriarty, Boris Eiteneer, Mikhail Goldenberg, C. Thomas Bowman, Ronald K. Hanson, Soonho Song, William C. Gardiner, Jr., Vitali V. Lissianski, and Zhiwei Qin. In: http://www.me.berkeley.edu/gri_mech/.
 47. BIOVIA DS. Materials Studio 2017. In: . Dassault Systèmes (2017).
 48. Aktulga HM, Fogarty JC, Pandit SA, Grama AY. Parallel reactive molecular dynamics: Numerical methods and algorithmic techniques. *Parallel Computing* **38**, 245-259 (2012).
 49. Chenoweth K, Van Duin AC, Goddard WA. ReaxFF reactive force field for molecular dynamics simulations of hydrocarbon oxidation. *J Phys Chem A* **112**, 1040-1053 (2008).
 50. O'Boyle NM, Banck M, James CA, Morley C, Vandermeersch T, Hutchison GR. Open Babel: An open chemical toolbox. *Journal of cheminformatics* **3**, 33 (2011).
 51. Tarjan R. Depth-first search and linear graph algorithms. *SIAM journal on computing* **1**, 146-160 (1972).
 52. Rupp M, Tkatchenko A, Müller K-R, Von Lilienfeld OA. Fast and accurate modeling of molecular atomization energies with machine learning. *Phys Rev Lett* **108**, 058301 (2012).
 53. Hloucha M, Deiters U. Fast coding of the minimum image convention. *Mol Simul* **20**, 239-244 (1998).
 54. Sculley D. Web-scale k-means clustering. In: *Proceedings of the 19th international conference on World wide web* (ed[^](eds). ACM (2010).
 55. Zhang L, Lin D-Y, Wang H, Car R, Weinan E. Active learning of uniformly accurate interatomic potentials for materials simulation. *Physical Review Materials* **3**, 023804 (2019).
 56. Frisch M, *et al.* Gaussian 16, revision A. 03. *Gaussian Inc, Wallingford CT*, (2016).
 57. Haoyu SY, He X, Li SL, Truhlar DG. MN15: A Kohn–Sham global-hybrid exchange–correlation density functional with broad accuracy for multi-reference and single-reference systems and noncovalent interactions. *Chem Sci* **7**, 5032-5051 (2016).
 58. Wang H, Zhang L, Han J, Weinan E. DeePMD-kit: A deep learning package for many-body potential energy representation and molecular dynamics. *Comput Phys Commun* **228**, 178-184 (2018).
 59. He K, Zhang X, Ren S, Sun J. Deep residual learning for image recognition. In: *Proceedings of the IEEE conference on computer vision and pattern recognition* (2016).

